THE JOURNAL OF BIOLOGICAL CHEMISTRY
Vol. 279, No. 47, Issue of November 19, pp. 49131–49137, 2004
Printed in U.S.A.

Structural and Dynamic Independence of Isopeptide-linked RanGAP1 and SUMO-1*[S]

Received for publication, July 30, 2004, and in revised form, August 26, 2004
Published, JBC Papers in Press, September 7, 2004, DOI 10.1074/jbc.M408705200

Matthew S. Macauley‡, Wesley J. Errington‡, Mark Okon‡, Manuela Schärpf‡, Cameron D. Mackereth‡, Brenda A. Schulman§, and Lawrence P. McIntosh‡¶

From the ‡Department of Biochemistry and Molecular Biology, the Department of Chemistry, and the Biotechnology Laboratory, University of British Columbia, Vancouver, British Columbia V6T 1Z3, Canada and the §Departments of Structural Biology and Genetics/Tumor Cell Biology, St. Jude Children's Research Hospital, Memphis, Tennessee 38105

Although sumoylation regulates a diverse and growing number of recognized biological processes, the molecular mechanisms by which the covalent attachment of the ubiquitin-like protein SUMO can alter the properties of a target protein remain to be established. To address this question, we have used NMR spectroscopy to characterize the complex of mature SUMO-1 with the C-terminal domain of human RanGAP1. Based on amide chemical shift and ^{15}N relaxation measurements, we show that the C terminus of SUMO-1 and the loop containing the consensus sumoylation site in RanGAP1 are both conformationally flexible. Furthermore, the overall structure and backbone dynamics of each protein remain unchanged upon the covalent linkage of Lys^{524} in RanGAP1 to the C-terminal Gly^{97} of SUMO-1. Therefore, SUMO-1 and RanGAP1 behave as "beads-on-a-string," connected by a flexible isopeptide tether. Accordingly, the sumoylation-dependent interaction of RanGAP1 with the nucleoporin RanBP2 may arise through the bipartite recognition of both RanGAP1 and SUMO-1 rather than through a new binding surface induced in either individual protein upon their covalent linkage. We hypothesize that this conformational flexibility may be a general feature contributing to the recognition of ubiquitin-like modified proteins by their downstream effector machineries.

Post-translational modification by ubiquitin and ubiquitin-like proteins (Ubls)[1] is an essential cellular regulatory mechanism, allowing rapid and reversible control of a target protein's function by altering its half-life, sub-cellular localization, enzymatic activity, protein-protein interactions, or other properties (see Ref. 1 for a recent review). Ubiquitin itself can direct its targets to a number of different fates, including proteasomal degradation and membrane protein transport (2). Ubls also control critical cellular functions. For example, NEDD8 activates SCF and related ubiquitin ligases, ISG15/UCRP is induced during in the antiviral interferon response, Apg12p and Apg8p regulate the autophagy pathway, and Hub1p modifies cell polarity factors. The Ubl SUMO regulates a growing number of recognized proteins involved in the cell cycle, DNA repair, the stress response, nuclear transport, transcription, and signal transduction (for recent reviews see Refs. 1 and 3–6).

The first protein shown to be post-translationally modified with SUMO is the RanGTPase-activating protein RanGAP1 (7, 8). In higher eukaryotes, the cellular localization of RanGAP1 is regulated by sumoylation of its C-terminal domain. During interphase, RanGAP1 is bound to the cytoplasmic side of the nuclear pore complex via a sumoylation-dependent interaction with the IR domain of the large nucleoporin RanBP2/Nup358 (9). This localization is required to help create and maintain the spatial gradient of the GTP-bound *versus* GDP-bound forms of Ran across the nuclear envelope necessary to drive nucleocytoplasmic transport (10). During mitosis, the nuclear envelope breaks down, destroying the Ran-GTP gradient. However, another Ran-GTP gradient is established to help mitotic spindle assembly. Once again, in vertebrates a requisite for the formation of this gradient is the localization of sumoylated RanGAP1 in complex with RanBP2 at the mitotic spindle and with the kinetochores (11).

After proteolytic cleavage of nascent SUMO to reveal a C-terminal Gly-Gly motif, sumoylation proceeds with the attachment of the mature protein via its C terminus to a cysteine residue in the SAE2 subunit of the heterodimeric E1 activating enzyme SAE1/SAE2. Formation of the thiolester bond is driven energetically by ATP hydrolysis. This reaction is followed by transesterification of SUMO to Cys^{93} on UBC9, the E2 conjugating enzyme. Although E3 ligating enzymes, which facilitate sumoylation, have been identified recently, UBC9 is sufficient for transferring SUMO to target proteins such as RanGAP1, at least *in vitro* (4–6). The final product is a covalent isopeptide linkage joining the C-terminal carboxyl of SUMO with the side

* This research was supported by grants from the National Cancer Institute of Canada with funds from the Canadian Cancer Society (to L. P. M.) as well as National Institutes of Health Grant R01GM69530 (B. A. S). Instrument support was provided by the Government of Canada's Network of Centres of Excellence Program supported by the Canadian Institutes of Health Research (CIHR) and the Natural Sciences and Engineering Research Council (NSERC) through the Protein Engineering Network of Centres of Excellence (PENCE, Inc.). The costs of publication of this article were defrayed in part by the payment of page charges. This article must therefore be hereby marked "*advertisement*" in accordance with 18 U.S.C. Section 1734 solely to indicate this fact.

[S] The on-line version of this article (available at http://www.jbc.org) contains additional data on $RanGAP1_c$ and $SUMO\text{-}1_{gg}$ in the form of supplemental Figs. S1 and S2 and Table S1.

The assigned chemical shift list has been deposited in the BioMagResBank under accession numbers 6304, 6305, and 6306.

¶ A Canadian Institutes of Health Research Scientist and to whom correspondence should be addressed: Dept. of Biochemistry, 2146 Health Sciences Mall, University of British Columbia, Vancouver, British Columbia V6T 1Z3, Canada. Tel.: 604-822-3341; Fax: 604-822-5227; E-mail: mcintosh@otter.biochem.ubc.ca.

[1] The abbreviations used are: Ubl, ubiquitin-like protein; $RanGAP1_c$, residues 420–587 of human RanGAP1 plus an N-terminal Gly-Ser-His tripeptide; $SUMO\text{-}1_{gg}$, residues 1–97 of human SUMO-1 plus an N-terminal Gly-Ser-His tripeptide; E1, Ubl-activating enzyme; E2, Ubl-conjugating enzyme; E3, Ubl-protein isopeptide ligase; HSQC, heteronuclear single quantum coherence; NOE, nuclear Overhauser effect; NOESY, NOE spectroscopy; TOCSY, total correlation spectroscopy; τ_c, correlation time.

chain amino group of a lysine in the target protein. There are three paralogs of SUMO present in humans, of which SUMO-2 and SUMO-3, like ubiquitin, can subsequently form poly-sumoylated chains, whereas SUMO-1 cannot (12). The residue targeted by SUMO-1 in mouse RanGAP1 is Lys^{526} (Lys^{524} in the human ortholog) (13), which lies in a $\psi KXE/D$ sumoylation consensus motif (ψ represents a large branched hydrophobic residue (Ile, Val, or Leu), and *X* is any amino acid) (14, 15). The crystal structure of the C-terminal domain of mouse RanGAP1 in complex with the human SUMO E2 conjugating enzyme, UBC9, revealed the molecular determinants for recognition of this motif (16).

In contrast to a rapidly growing understanding of the enzymatic mechanisms by which Ubls are specifically conjugated to their target proteins (16–18), remarkably little is known about the structural consequences of these post-translational modifications. Studies of di-ubiquitin conjugates revealed interactions between the members of a Lys^{48}-linked pair, but not between those joined at Lys^{63} (19–21). The crystal structure of the MoaD:MoaE molybdopterin synthase complex may also shed light on the consequences of Ubl modification. Although MoaD and MoaE are not naturally linked, in this complex the C-terminal glycine of MoaD, which resembles ubiquitin, is isopeptide-bonded to a lysine in MoaE (22). The structure also revealed extensive non-covalent interactions between MoaD and MoaE, resulting in conformational changes in the interfacial regions of both proteins (23). These studies raise the key question as to whether Ubl modification of natural targets also involves significant non-covalent Ubl-target interactions leading to conformational changes in either protein or whether the Ubl is simply covalently linked to the target by a flexible tether (6). For example, it has been hypothesized that sumoylation exposes or creates a new binding surface on RanGAP1 for specific recognition by RanBP2, because neither unmodified SUMO-1 nor RanGAP1 interact with this nucleoporin (13).

To examine the related concepts regarding the structural and dynamic determinants for the sumoylation of target proteins and the consequences of this post-translational modification, we used NMR spectroscopy to characterize human SUMO-1 and the C-terminal domain of RanGAP1 in their free and covalently linked forms. Based on these studies, we confirm that the target lysine of RanGAP1, as well as the C terminus of mature SUMO-1, lie within mobile regions of the two proteins. Furthermore, we demonstrate that, upon sumoylation, RanGAP1 and SUMO-1 behave as "beads-on-a-string" joined by a flexible isopeptide tether and that their structures and local dynamic features do not change significantly beyond the site of this covalent linkage. These results discount a model of a sumoylation-dependent conformational change in RanGAP1 and/or SUMO-1 to mediate RanBP2 binding.

EXPERIMENTAL PROCEDURES

DNA Constructs—Genes encoding residues 1–97 of SUMO-1 (denoted $SUMO\text{-}1_{gg}$), residues 420–587 of RanGAP1 (denoted $RanGAP1_c$), and full-length UBC9 were PCR cloned from a human HeLa cell QUICK-Clone cDNA library (Clontech Laboratories) into the pET28a expression vector (Novagen) using NdeI and XhoI restriction enzyme sites. The resulting constructs contained an N-terminal His_6 tag with a thrombin cleavage site such that a Gly-Ser-His extension remained after proteolytic processing. The clone of the yeast E1 activating enzyme (AOS1/UBA1) was generated as described (24).

Protein Expression and Purification—Proteins were expressed using *Escherichia coli* BL21(λ DE3) cells grown in Luria-Bertani media or in M9 media containing $^{15}NH_4Cl$ and/or $^{13}C_6$-glucose according to standard protocols (25). Post-induction cells were collected by centrifugation, re-suspended in nickel column binding buffer (500 mM NaCl, 50 mM HEPES, 5 mM imidazole, and 5% glycerol, pH 7.5), lysed with a French Press, and sonicated. The cell debris was pelleted, and the resultant supernatant was filtered through a 0.8-μm cellulose acetate membrane (Nalgene) directly onto a nickel-affinity column (HiTrap; Amersham Biosciences). The column was washed with 125 ml of wash buffer (as binding plus 60 mM imidazole), and proteins were eluted with elution buffer (as binding plus 250 mM imidazole). The eluted fractions were pooled and dialyzed overnight into 10 mM NaCl, 50 mM Tris, and 2 mM β-mercaptoethanol (pH 7.5) in preparation for sumoylation reactions or into 100 mM KCl, 10 mM potassium phosphate, 5 mM dithiothreitol, and 0.1 mM EDTA at pH 6.0 or 6.5 for NMR spectroscopy. When necessary to remove the His_6 tag, thrombin was included during the dialysis step and subsequently inactivated with *p*-aminobenzamidine beads (Sigma). Talon metal affinity resin (Clontech) was added in a batch method to remove the cleaved His_6 tag. The final sample concentrations were determined by UV light absorbance using a predicted ϵ_{280} of 29,400 M^{-1} cm^{-1} for UBC9 and an ϵ_{278} of 3,840 M^{-1} cm^{-1} for $SUMO\text{-}1_{gg}$ and $RanGAP1_c$. SDS-PAGE and electrospray ionization mass spectroscopy were used to confirm the mass and purity of each protein.

In Vitro Sumoylation and Purification of the $RanGAP1_c$:$SUMO\text{-}1_{gg}$ Complex—Sumoylation reactions, monitored by SDS-PAGE, were carried out overnight at 37 °C using 100-ml solutions containing ~50 μM $RanGAP1_c$, 50 μM $SUMO\text{-}1_{gg}$, 10 μM UBC9, 5 μM AOS1/UBA1, 10 mM ATP, 5 mM $MgCl_2$, 50 mM Tris, 10 mM NaCl, and 5 mM dithiothreitol (pH 7.5). To prepare the $^{15}N\text{-}RanGAP1_c$:$SUMO\text{-}1_{gg}$ complex, the His_6 tag was initially cleaved off all the components except $SUMO\text{-}1_{gg}$. For the $^{15}N\text{-}SUMO\text{-}1_{gg}$:$RanGAP1_c$ complex, the His_6 tag was cleaved off all the components except $RanGAP1_c$. Each reaction mixture was diluted into nickel column binding buffer and purified as described above over a nickel-affinity column. After elution, the pooled product was loaded onto a Fractogel® SO_3^- column (Merck) in 20 mM potassium phosphate and 5 mM β-mercaptoethanol (pH 5.5) and eluted over a 120-min period with a 0–750 mM NaCl gradient in this buffer to further purify the desired complex. The resulting $^{15}N\text{-}RanGAP1_c$:$SUMO\text{-}1_{gg}$ and $^{15}N\text{-}SUMO\text{-}1_{gg}$:$RanGAP1_c$ were dialyzed into 100 mM KCl, 10 mM potassium phosphate, 5 mM dithiothreitol, and 0.1 mM EDTA at pH 6.0 and 6.5, respectively. Thrombin was included during dialysis to remove the His_6 tag as described above. The final protein complexes were concentrated by ultrafiltration (Millipore) to 0.65 and 0.5 mM, respectively, and D_2O was added to ~10%. Both preparations had an ~33% yield. SDS-PAGE and electrospray ionization mass spectroscopy were used to confirm the mass of the complexes. A small amount of unmodified $RanGAP1_c$ and $SUMO\text{-}1_{gg}$, as well as residual His_6-tagged complex, was observed in each preparation.

NMR Spectroscopy—Protein samples were in 100 mM KCl, 10 mM potassium phosphate, 5 mM dithiothreitol, 0.1 mM EDTA, and ~10% D_2O at pH 6 or 6.5. Spectra for labeled $SUMO\text{-}1_{gg}$ were recorded at 17 °C on a Varian Unity 500 MHz spectrometer. Spectra for labeled $RanGAP1_c$ and UBC9 were recorded at 17 and 30 °C on a Varian Inova 600 MHz spectrometer. The reduced temperature was used to limit protein aggregation and/or degradation (26, 27). The $^1H^N$, ^{15}N, $^{13}C\alpha$, and $^{13}C\beta$ assignments for $^{13}C/^{15}N\text{-}RanGAP1_c$ were obtained through standard triple resonance NMR experiments (28). Amide $^1H^N$ and ^{15}N assignments for $^{15}N\text{-}SUMO\text{-}1_{gg}$, $^{15}N\text{-}UBC9$, $^{15}N\text{-}RanGAP1_c$:$SUMO\text{-}1_{gg}$, and $^{15}N\text{-}SUMO\text{-}1_{gg}$:$RanGAP1_c$ were confirmed using three-dimensional ^{15}N-NOESY and TOCSY-HSQC spectra. Assignments for residues 1–97 of $SUMO\text{-}1_{gg}$ (26, 27) and UBC9 (29) were based on those reported previously. NMR-monitored titrations of $^{15}N\text{-}RanGAP1_c$ (pH 6.0) were carried out with UBC9 at 30 °C or $SUMO\text{-}1_{gg}$ at 17 °C, whereas those of $^{15}N\text{-}SUMO\text{-}1_{gg}$ (pH 6.5) with $RanGAP1_c$ were recorded at 17 °C, and those of $^{15}N\text{-}UBC9$ (pH 6.5) with $RanGAP1_c$ were recorded at 30 °C. In each case, the experiment began with 500 μl of 400 μM labeled protein to which aliquots of 2 mM unlabeled protein in the same buffer were added in 10 steps to a final molar excess of 4:1. Amide ^{15}N T_1 and T_2, and heteronuclear $^1H\text{-}^{15}N$ NOE relaxation measurements were recorded as described (30). Spectral processing, resonance assignments, and relaxation analyses were carried out using NMRPipe (31), SPARKY 3 (32), and Tensor2 (33). The chemical shift assignments of $^{13}C/^{15}N\text{-}RanGAP1_c$, $^{15}N\text{-}SUMO\text{-}1_{gg}$, and $^{15}N\text{-}RanGAP1_c$:$SUMO\text{-}1_{gg}$ have been deposited in the BioMagRes Bank (www.bmrb.wisc.edu/) under accession numbers 6305, 6304, and 6305, respectively.

RESULTS

The Target Lysine for Sumoylation of $RanGAP1_c$ by UBC9 Lies in a Flexible Loop—Resonances from the backbone ^1H, ^{13}C, and ^{15}N nuclei in the C-terminal domain of human RanGAP1 were assigned by established NMR methods (Fig. 1*A* and supplemental Fig. S1, available in the on-line version of this article). Based on the measured $^1H^N$, ^{15}N, $^{13}C^\alpha$, $^{13}C^\beta$, and $^{13}C'$ chemical shifts, the secondary structure of this protein consists

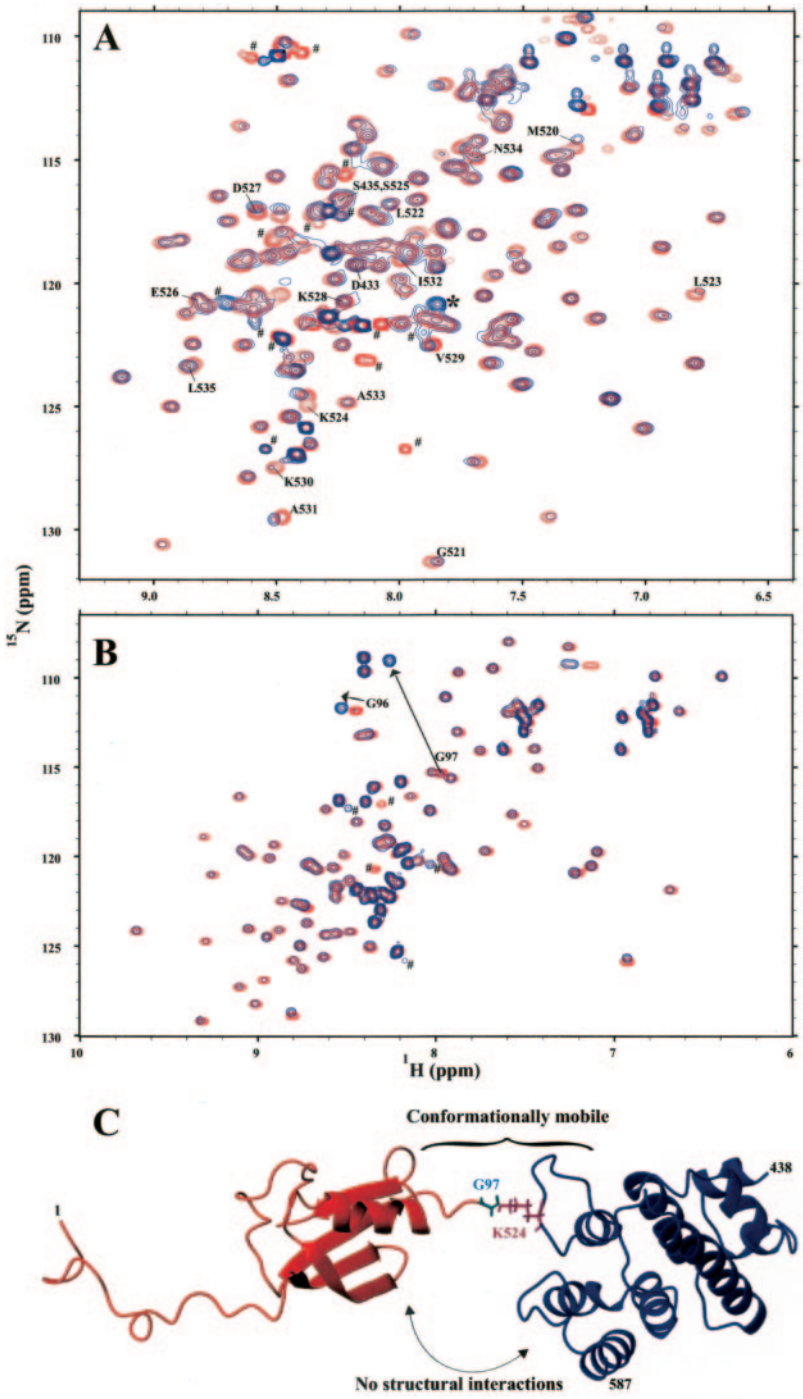

FIG. 1. **Sumoylation of RanGAP1$_c$ leads to no significant NMR chemical shift changes and, hence, no structural perturbations in either protein.** *A*, overlaid ^{1}H-^{15}N HSQC spectra of ^{15}N-RanGAP1$_c$ (*red*) and ^{15}N-RanGAP1$_c$:SUMO-1$_{gg}$ (*blue*) at pH 6.0 and 17 °C. Peaks from residues 520–535 are labeled, and the *asterisk* (*) indicates the new isopeptide between Lys^{524} of RanGAP1$_c$ and Gly^{97} of SUMO-1$_{gg}$. The signal from Lys^{524} in sumoylated RanGAP1$_c$ overlaps with that from the free protein but is not seen at this contour level. *B*, overlaid ^{1}H-^{15}N HSQC spectra of ^{15}N-SUMO-1$_{gg}$ (*red*) and ^{15}N-SUMO-1$_{gg}$:RanGAP1$_c$ (*blue*) at pH 6.5 and 17 °C. The *arrows* indicate the changes in the chemical shifts of Gly^{96} and Gly^{97} due to covalent bonding to RanGAP1$_c$. Signals from residual His$_6$ tag and/or minor contaminants are indicated with a *pound symbol* (#). Subtle spectral shifts arise due to small differences in pH or ionic strength between the protein samples, as demonstrated by control titration measurements. Fully annotated spectra are provided in Supplemental Fig. S1, available in the on-line version of this article. *C*, beads-on-a string model of RanGAP1$_c$:SUMO-1$_{gg}$ linked by a flexible isopeptide tether. The ribbon diagram of SUMO-1$_{gg}$ (*red*) is from the NMR-derived structure of the full-length nascent protein (Protein Data Bank accession code 1AR5), whereas that of human RanGAP1$_{gg}$ (*blue*) was generated (46) using the x-ray crystallographic co-ordinates of the mouse ortholog in complex with UBC9 (Protein Data Bank accession code 1KPS). Gly^{97} of SUMO-1$_{gg}$ (*cyan*) and Lys^{524} of RanGAP1$_c$ (*purple*) are positioned to form an isopeptide bond. The two proteins are structurally independent, and the isopeptide bond, as well as the backbone of surrounding residues at the C terminus of SUMO-1$_{gg}$ and within the H6-H7 loop of RanGAP1$_c$, are conformationally mobile on the sub-nanosecond time scale. Because of these dynamic properties, the model is only a snapshot of a large ensemble of possible orientations for the two proteins. Single letter amino acid abbreviations are used with position numbers throughout the figure.

of nine α-helixes and matches that found in the crystal structure of the closely related mouse protein (82% identical residues) (16).

The dynamic properties of ^{15}N-RanGAP1$_c$ were probed using ^{15}N relaxation experiments, which provide a measure of both the global rotational diffusion of a protein as well as the local mobility of its polypeptide backbone on a residue-specific basis (34). From the T_1 and T_2 lifetimes of amides within the helical core of RanGAP1$_c$, an effective correlation time (τ_c) of 12.5 ± 0.1 ns was determined for its global tumbling at 17 °C. This value is within the range expected for a monomeric protein of 18.7 kDa at this temperature (35). In parallel, insights into the internal mobility of RanGAP1$_c$ were obtained from steady-state ^{1}H-^{15}N NOE data. The heteronuclear NOE is a sensitive indicator of dynamics on a sub-nanosecond time scale with values at a ^{15}N frequency of 50.7 MHz ranging from 0.82 for rigid ^{1}H-^{15}N groups to −3.6 for those showing unrestricted mobility (34). As documented in Fig. 2*A* (and in supplemental Table S1 in the on-line version of this article), amides within the ordered helices of the C-terminal domain of ^{15}N-RanGAP1$_c$ have an average of ^{1}H-^{15}N NOE of 0.77 ± 0.06, whereas the 12 residues in the disordered region preceding this domain have negative NOE values. More importantly, residues 504–508 and 520–535 between helices H5-H6 and H6-H7, respectively, show reduced ^{1}H-^{15}N NOE values (averages of 0.56 ± 0.09 and 0.61 ± 0.13, respectively) that are indicative of enhanced backbone mobility relative to the remainder of the structured C-terminal domain. The latter of these flexible regions corresponds to a large exposed loop in the crystal structure of mouse RanGAP1$_c$ and contains the consensus sumoylation motif Leu-Lys^{524}-Ser-Glu

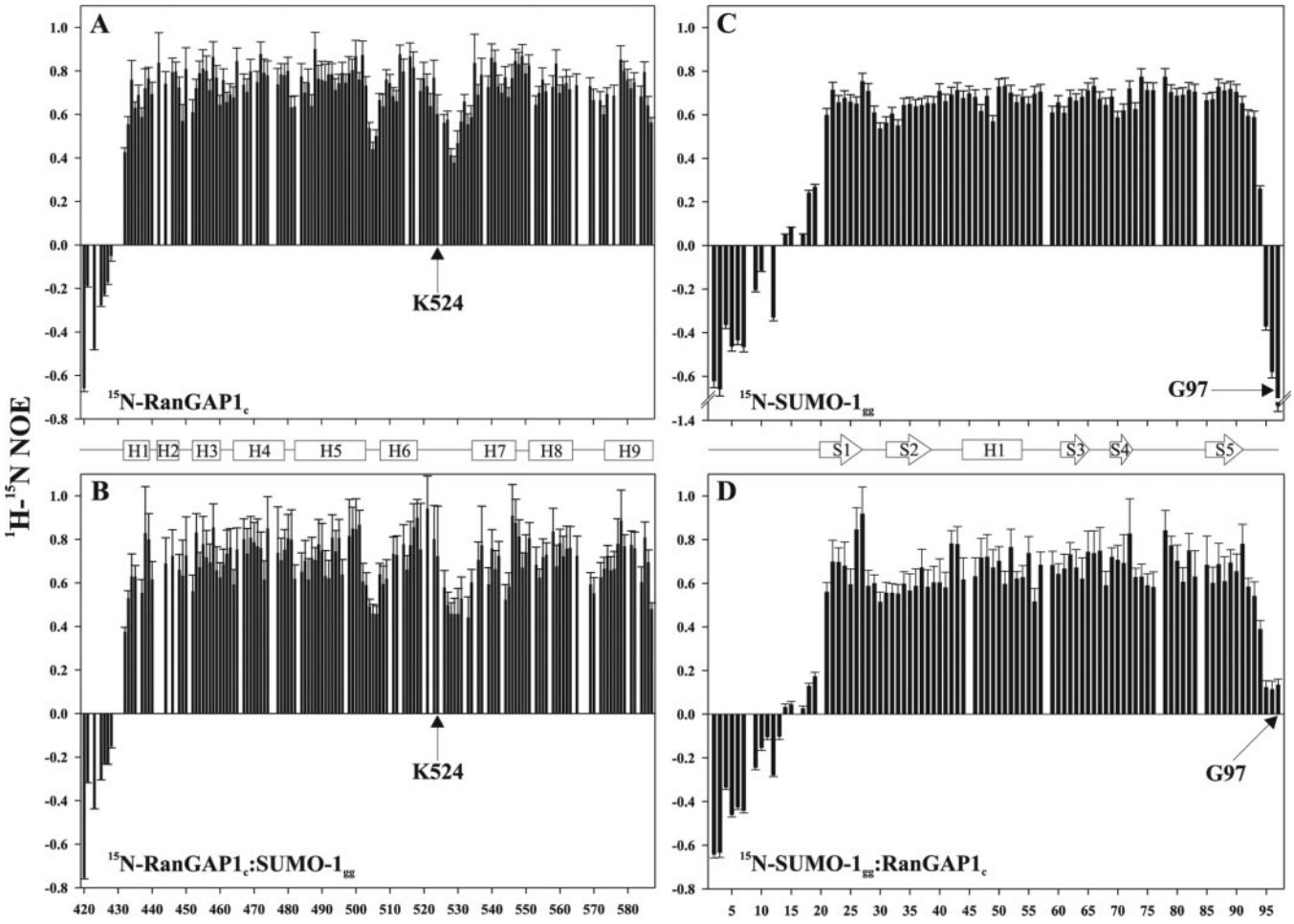

FIG. 2. **Characterizing the internal backbone dynamics of ^{15}N-RanGAP1$_c$ (*A*), ^{15}N-RanGAP1$_c$:SUMO-1$_{gg}$ (*B*), ^{15}N-SUMO-1$_{gg}$ (*C*), and ^{15}N-SUMO-1$_{gg}$:RanGAP1$_c$ (*D*) by steady-state ^{1}H-^{15}N NOE relaxation measurements.** Decreasing ^{1}H-^{15}N NOE values indicate increasing amide mobility on the sub-nanosecond time scale. *A*, in addition to its disordered N terminus, the loops between helices H5-H6 and H6-H7 in ^{15}N-RanGAP1$_c$, which include the target Lys^{524} (*K524*), are conformationally flexible relative to the ordered helical core of the protein. *B*, upon sumoylation, the fast local dynamic features of ^{15}N-RanGAP1$_c$:SUMO-1$_{gg}$ do not change significantly. *C*, the N and C termini of ^{15}N-SUMO-1$_{gg}$, including Gly^{97} (*G97*), are also conformationally flexible. *D*, upon linkage to RanGAP1$_c$, the C terminus of ^{15}N-SUMO-1$_{gg}$ remains mobile albeit dampened relative to the free state, whereas internal dynamic properties of the remainder of the protein are essentially unperturbed. The data for ^{15}N-RanGAP1$_c$ and ^{15}N-RanGAP1$_c$:SUMO-1$_{gg}$ were averaged from two measurements. The increased *error bars* for the complexes *versus* free proteins reflect the decreased signal-to-noise ratio in the spectra of the larger molecules at lower sample concentrations. Missing data points correspond to prolines or residues with severe spectral overlap. These data are provided in supplemental Table S1, available in the on-line version of this article.

(16). The amide ^{1}H-^{15}N NOE value of Lys^{524} within this loop is 0.60 ± 0.09.

To confirm that the consensus motif in the flexible H6-H7 loop of human RanGAP1$_c$ is the target of UBC9-mediated sumoylation and to verify that a known intermolecular interface for RanGAP1$_c$ can be detected by NMR methods, the interaction between these two proteins in solution was investigated. Specifically, ^{1}H-^{15}N HSQC spectra of either ^{15}N-labeled RanGAP1$_c$ or UBC9 were recorded upon titration with the unlabeled partner (supplemental Fig. S2, available in the on-line version of this article). The chemical shifts and relaxation properties of a ^{1}H-^{15}N group are highly sensitive to its local environment, and, thus, selective perturbations in the HSQC spectrum of a protein provide a means to identify even subtle conformational changes such as those occurring at interaction surfaces. Upon titration, residues in ^{15}N-RanGAP1$_c$ clustering near helix H6 and the loops between H6-H7 (including Lys^{524}) and H8-H9 showed selective loss of intensity. A similar behavior was observed for residues in ^{15}N-UBC9 near helix H3, strands S6 and S7, and the catalytic Cys^{93}. These regions correspond very well with the intermolecular interface observed in the crystal complex of mouse RanGAP1$_c$ and human UBC9 in which the target lysine from this consensus motif is bound in close proximity to the active site cysteine of the E2 conjugating enzyme (16). Furthermore, based on the NMR titration data, including the observation of selective conformational exchange broadening, we estimate a dissociation constant (K_d) <10 μM for this protein complex. This K_d value is consistent with that of 0.5 μM determined for human UBC9 and RanGAP1$_c$ by isothermal titration calorimetry (36). Thus, NMR methods accurately detect a previously characterized protein-protein interaction involving RanGAP1$_c$. Parenthetically, this K_d is markedly lower than those in the millimolar range reported for peptide models of sumoylation sites from p53 and c-Jun (37) and supports the hypothesis that RanGAP1$_c$ is an efficient substrate for UBC9 because of the significant interaction surfaces between these two proteins.

The C Terminus of SUMO-1$_{gg}$ Is Conformationally Dynamic—The assigned ^{1}H-^{15}N HSQC spectrum of the biologically active form of human SUMO-1 (residues 1–97) is presented in Fig. 1*B*. Consistent with structural and relaxation studies reported for the nascent protein (26, 27), residues 1–20 and 94–97 at both termini of mature SUMO-1$_{gg}$ are conformationally mobile on the sub-nanosecond time scale as evidenced by reduced ^{1}H-^{15}N

NOE values (Fig. 2*C*). In addition, based on the ^{15}N T_1 and T_2 relaxation of amides within the structured core of the protein, the effective τ_c for the global tumbling of SUMO-1_{gg} (11.4 kDa) at 17 °C is 8.6 ± 0.1 ns.

RanGAP1$_c$ and SUMO-1$_{gg}$ Do Not Interact Non-covalently—To examine if RanGAP1$_c$ and SUMO-1_{gg} associate in solution, reciprocal NMR-monitored titrations of one unlabeled and one ^{15}N-labeled protein were performed. In both cases, the ^1H-^{15}N HSQC spectra of the labeled protein showed no selective intensity or chemical shift perturbations upon titration with a 4-fold molar excess of unlabeled partner (final concentration ratios, 220 to 890 μM; data not shown). Thus, unlike the case of UBC9, free RanGAP1$_c$ and SUMO-1_{gg} do not appreciably interact in a non-covalent manner.

The Structure and Dynamics of RanGAP1$_c$ Are Unperturbed upon Sumoylation—Milligram quantities of isopeptide-linked RanGAP1$_c$:SUMO-1_{gg} were prepared using a large scale *in vitro* sumoylation reaction. The reaction was carried out with only one of RanGAP1$_c$ or SUMO-1_{gg} ^{15}N-labeled to allow the selective detection of signals from that protein within the covalent complex. Although an expression system for generating SUMO-1 modified proteins in *E. coli* has been developed (38), such selective isotopic labeling would not be possible using this approach. To facilitate purification of the complex by nickel-affinity chromatography, while minimizing any potential background signal from the unmodified ^{15}N-protein, only the unlabeled protein in the reaction mixture carried a His_6 tag. The tag was removed proteolytically after isolation of the complex.

The ^1H-^{15}N HSQC spectrum of ^{15}N-RanGAP1$_c$:SUMO-1_{gg} overlaps closely with that of free ^{15}N-RanGAP1$_c$ (Fig. 1*A*). Given the exquisite sensitivity of amide chemical shifts to local environment, this finding clearly indicates that the overall structure of RanGAP1$_c$ is not significantly perturbed upon covalent modification, nor does a specific interaction occur with SUMO-1_{gg}. However, detailed inspection of the HSQC spectrum of the complex reveals that signals from residues 519–534 are relatively weakened, suggestive of localized millisecond time scale conformational exchange broadening due to the tethering of SUMO-1_{gg} to this loop region. In addition, a strong new peak at 7.85 and 121.0 ppm in ^1H and ^{15}N, respectively, is observed in the spectrum of ^{15}N-RanGAP1$_c$:SUMO-1_{gg}. This signal was assigned to the isopeptide amide group based on interprotein ^1H-^1H NOE interactions involving the $^1H^{\zeta}$ of Lys^{524} in RanGAP1$_c$ and the $^1H^{\alpha}$ and $^1H^N$ of Gly97 in SUMO-1_{gg} (Fig. 3).

Paralleling the lack of structural perturbations, ^1H-^{15}N NOE measurements reveal that the fast internal dynamics of the backbone of RanGAP1$_c$ are not significantly changed upon sumoylation (Fig. 2*B*). In particular, the H6-H7 loop region containing Lys^{524} continues to exhibit reduced NOE values indicative of local conformational mobility (0.72 ± 0.23 for Lys^{524} and an average of 0.59 ± 0.16 for residues 520–535). Moreover, the isopeptide $^{15}N^{\zeta}$ has a heteronuclear NOE value of 0.23 ± 0.06, demonstrating that the linkage is also very flexible on a sub-nanosecond time scale. Finally, as expected because of an increase in mass, ^{15}N T_1 and T_2 relaxation experiments yielded a slower effective global τ_c of 18.1 ± 0.2 ns at 17 °C for the tumbling of RanGAP1$_c$ within the sumoylated 30.1 kDa complex.

The Structure and Dynamics of SUMO-1$_{gg}$ Are Unperturbed upon Attachment to RanGAP1$_c$—Complementary to the previous experiments, the properties of ^{15}N-SUMO-1_{gg}:RanGAP1$_c$ were compared with those of ^{15}N-SUMO-1_{gg}. The ^1H-^{15}N HSQC spectrum of this protein within the sumoylated complex overlaps very well with that of the unmodified state (Fig. 1*B*), demonstrating that the structure of SUMO-1_{gg} is also not perturbed upon covalent linkage to RanGAP1. Chemical shift changes are only observed for Gly^{96} and Gly^{97}, as is expected for the conversion of the charged C terminus of SUMO-1_{gg} to a neutral isopeptide. Indeed, the amide chemical shifts of Gly^{97} in ^{15}N-SUMO-1_{gg}:RanGAP1$_c$ resemble those reported for nascent SUMO-1 with it native C-terminal sequence (His-Ser-Thr-Val^{101}) followed by a His_6 tag (27). Similarly, ^{15}N relaxation measurements reveal an increase in the effective τ_c for global tumbling of ^{15}N-SUMO-1_{gg} to 13.6 ± 0.2 ns at 17 °C upon covalent complex formation, yet no overall changes in the pattern of fast internal backbone dynamics are exhibited by this protein (Fig. 2*D*). Although the motions of the Thr^{95}-Gly^{97}, as reflected by ^1H-^{15}N NOE values, are dampened relative to the free protein because of their direct attachment to RanGAP1$_c$, these residues remain flexible relative to the well ordered core of SUMO-1_{gg}.

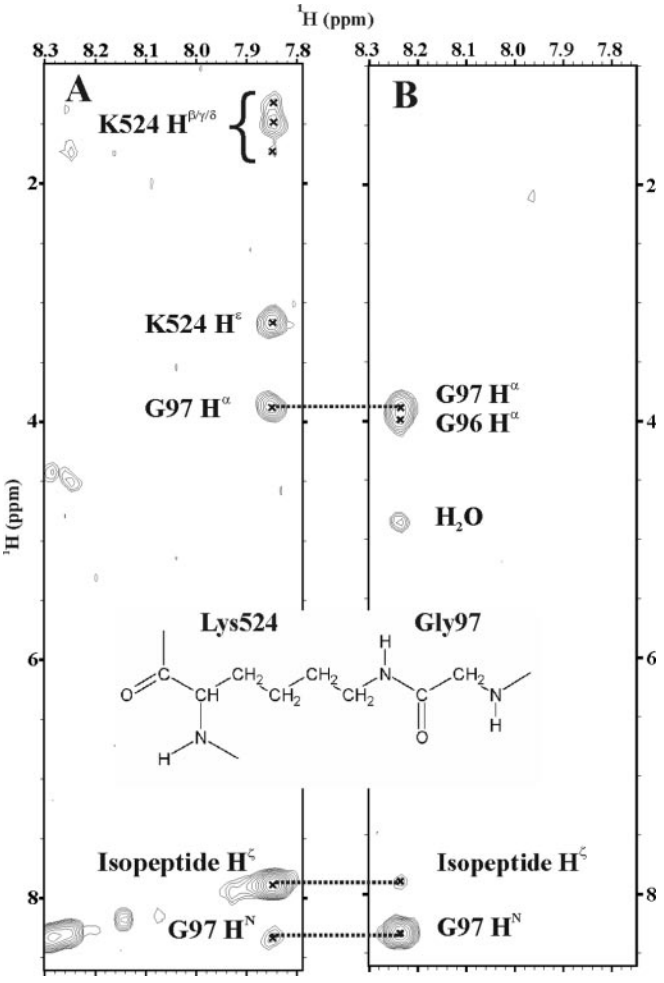

FIG. 3. **Assignment of the ^1H-$^{15}N^{\zeta}$ resonances from the new isopeptide linkage between Lys^{524} (*K524*) of ^{15}N-RanGAP1$_c$ and Gly^{97} (*G97*) of SUMO-1_{gg}.** Shown are strip plots from the three-dimensional ^{15}N-NOESY-HSQC spectra of ^{15}N-RanGAP1$_c$:SUMO-1_{gg} at the ^{15}N chemical shift of the isopeptide $^{15}N^{H\zeta}$ (*A*) and of ^{15}N-SUMO-1_{gg}:RanGAP1$_c$ at the ^{15}N chemical shift of Gly^{97} (*B*).

DISCUSSION

Conformational Flexibility of Sumoylation Sites—As expected from previous studies of nascent SUMO-1 (26, 27), the residues C-terminal to the fifth β-strand of mature SUMO-1_{gg} are conformationally mobile. This flexibility may be critical for the proteolytic activation of SUMO-1 and the de-sumoylation of target proteins (39), as well as for SUMO-1_{gg} to bind to UBC9 while extending its C terminus to form a thiolester with the distal Cys^{93} (16, 29). Similarly, as was also revealed by ^{15}N

relaxation measurements, the sumoylation site in human $RanGAP1_c$ lies within a dynamic region corresponding to the exposed H6-H7 loop observed in the crystal structure of its mouse ortholog complexed with UBC9 (16). The accessibility and plasticity of this site is likely necessary for the Leu-Lys^{524}-Ser-Glu sequence of $RanGAP1_c$ to bind UBC9 in an extended conformation along a shallow surface adjacent to Cys^{93}. As hypothesized previously from studies of isolated peptide models of p53 and c-Jun sumoylation sites (37), this conformational flexibility may be a general feature of the regions in target proteins containing lysines to which SUMO is attached. A survey of characterized sumoylation sites indicates that many indeed fall within the unstructured N-terminal (*i.e.* histone H4, IκBα, and Sumo-2/3) or C-terminal (p53) tails of proteins or in internal regions linking structured domains (c-Jun and Sp100). However, exceptions may exist as evidenced by reported sumoylation sites within non-loop regions of the well structured PNT domain of Tel (40) and the RING domain of PML (41). It is possible that E3 SUMO ligases are required to facilitate the attachment of SUMO to such sites *in vivo*, as the Tel PNT domain is not sumoylated directly by UBC9 *in vitro*.[2]

RanGap:SUMO-1 Are Beads-on-a-String Connected via a Flexible Isopeptide Linker—Although the involvement of sumoylation in regulating several diverse biological processes is well documented, little is understood regarding the molecular mechanisms by which the attachment of SUMO mediates these cellular consequences (6). In cases such as IκBα and Mdm2, sumoylation appears to sterically compete with ubiquitinylation of the same target lysine to prevent proteolytic degradation (42, 43). However SUMO also plays an active role altering the interactions of target protein with other macromolecules. Examples include the sumoylation-dependent assembly of PML nuclear bodies (6), as well as the recruitment of histone deacetylase complexes by sumoylated Elk-1, resulting in transcriptional repression (44). The activity of an enzyme may also be sumoylation-dependent, as illustrated by the reduction in the DNA binding affinity of thymine-DNA glycosylase upon its covalent linkage to SUMO (45). As recently reviewed (6), two general, nonexclusive models can be envisioned by which sumoylation could affect the interactions of a target protein with another macromolecule in order to impart a cellular response: (i) upon covalent-linkage the conformation of the target protein and/or SUMO becomes altered, exposing or sequestering a specific recognition surface on one member of the pair; or (ii) as a tethered heterodimer, SUMO and the target protein co-operatively contribute determinants to a new multipartite binding interface.

A description of the structural and dynamic consequences of the covalent linkage of SUMO, ubiquitin, or any other Ubl to target proteins, as is required to distinguish these models, remains remarkably absent in the literature. To date, only two di-ubiquitins and a MoaD:MoaE molybdopterin synthase complex with a non-native isopeptide have been characterized *in vitro*. The attachment of the C-terminal Gly^{76} of one ubiquitin to the Lys^{48} of another, as is found in the polyubiquitinylation pathway leading to proteasomal degradation, results in a dynamic equilibrium involving a closed conformation between the two proteins that sequesters a hydrophobic interface (19, 20). In contrast, attachment through Lys^{63}, which acts as a specific signal in several non-degradative processes, leads to no structural perturbations in either member of the ubiquitin pair (21).

Using NMR spectroscopy we demonstrate that, similar to Lys^{63}-linked di-ubiquitin, the $RanGAP1_c$:$SUMO\text{-}1_{gg}$ complex is connected via a flexible isopeptide linkage with no significant structural interactions between the two proteins. This beads-on-a-string behavior (Fig. 1*C*) is based on a comparison of three properties of $RanGAP1_c$ and $SUMO\text{-}1_{gg}$ in complex *versus* free in solution. First, the ^1H-^{15}N HSQC spectrum of each selectively ^{15}N-labeled member of the complex overlaps very closely with that of the corresponding free protein, with the exception of changes in the intensities or chemical shifts of signals from residues immediately adjacent to the isopeptide bond. Thus, beyond these residues, the structure of neither protein is measurably perturbed upon their covalent linkage, nor is a defined interaction surface between the two proteins within the complex detected. Second, the isopeptide bond is very dynamic on a sub-nanosecond time scale as evidenced by a ^1H-^{15}N NOE value of ~0.2. Furthermore, the fast time scale conformational mobility of the flexible loop containing Lys^{524} in $RanGAP1_c$ does not markedly change upon sumoylation. The broadening of the resonances from residues 519 to 534 does, however, suggest some slower motions on a chemical shift (*i.e.* millisecond) time scale for this region to which $SUMO\text{-}1_{gg}$ is now covalently attached. Similarly, the C terminus of $SUMO\text{-}1_{gg}$ remains flexible in complex, although dampened relative to its free state because of hydrodynamic drag from the attached $RanGAP1_c$. Third, if the two proteins interacted to form a tightly associated pair, one would expect that the effective global τ_c measured for each would be similar and on the order of ~21 ns at 17 °C. This value, extrapolated from the correlation times determined for free $RanGAP1_c$ (18.7 kDa, 12.5 ns) and $SUMO\text{-}1_{gg}$ (11.4 kDa, 8.6 ns), corresponds to a globular heterodimer with a total molecular mass of 30.1 kDa. However, the τ_c values determined for $RanGAP1_c$ and $SUMO\text{-}1_{gg}$ in complex were 18.1 and 13.6 ns, respectively. The fact that these individual correlation times are both very different from one another and less than that expected for an intimate heterodimer indicates that the two molecules, for the most part, tumble independently within the covalently tethered complex.

It is well established that RanGAP1 requires the attachment of SUMO-1 in order to interact with RanBP2. Accordingly, sumoylation has been hypothesized to expose or create a new binding site on the C-terminal domain of RanGAP1 for RanBP2 (13). Based on the results of this study, the attachment of $SUMO\text{-}1_{gg}$ to $RanGAP1_c$ does not alter the structure or dynamics of either protein beyond the site of the isopeptide linkage. Thus, RanBP2 may cooperatively recognize determinants from both SUMO-1 and RanGAP1 when the two are topologically linked through a bipartite interface. The newly formed isopeptide group could also contribute to this interaction. Given that sumoylation consensus sites appear in general to fall within flexible or unstructured polypeptide segments, we speculate that this beads-on-a-string behavior may be a common feature of the diverse regulatory processes involving sumoylated proteins, as well as proteins post-translationally modified with other Ubls. The conformational flexibility that we observed in this study may translate into plasticity important for the binding of SUMO-modified targets by their downstream effector machineries. These dynamic properties may also allow a particular SUMO-modified protein to interact specifically with different binding partners.

Acknowledgments—We thank Gary Yalloway and Shouming He for assistance with mass spectrometry.

Note Added in Proof—Two recent papers provide insights into the recognition of SUMO (Song, J., Surrin, L. K., Wilkinson, T. A., Krontiris, T. G., and Chen, Y. (2004) *Proc. Natl. Acad. Sci. U. S. A.* **101,** 14373–14378) and RanBP2 (Pichler, A., Knipscheer, P., Saitoh, H., Sixma, T. K., and Melchior, F. (2004) *Nat. Struct. Mol. Biol.* **11,** 984–991).

[2] M. S. Macauley, W. J. Errington, M. Schärpf, C. D. Mackereth, and L. P. McIntosh, unpublished observation.

REFERENCES

1. Schwartz, D. C., and Hochstrasser, M. (2003) *Trends Biochem. Sci.* **28,** 321–328
2. Pickart, C. (2004) *Cell* **23,** 181–190
3. Hay, R. T. (2001) *Trends Biochem. Sci.* **26,** 332–333
4. Melchior, F., Schergaut, M., and Pichler, A. (2003) *Trends Biochem. Sci.* **28,** 612–618
5. Muller, S., Ledl, A., and Schmidt, D. (2004) *Oncogene* **23,** 1998–2008
6. Johnson, E. S. (2004) *Ann. Rev. Biochem.* **73,** 355–382
7. Matunis, M. J., Coutavas, E., and Blobel, G. (1996) *J. Cell Biol.* **135,** 1457–1470
8. Mahajan, R., Delphin, C., Guan, T., Gerace, L., and Melchior, F. (1997) *Cell* **88,** 97–107
9. Saitoh, H., Pu, R., Cavenagh, M., and Dasso, M. (1997) *Proc. Natl. Acad. Sci. U. S. A.* **94,** 3736–3741
10. Quimby, B. B., and Dasso, M. (2003) *Curr. Opin. Cell Biol.* **15,** 338–344
11. Joseph, J., Liu, S. T., Jablonski, S. A., Yen, T. J., and Dasso, M. (2004) *Curr. Biol.* **14,** 611–617
12. Tatham, M. H., Jaffray, E., Vaughan, O. A., Desterro, J. M., Botting, C. H., Naismith, J. H., and Hay, R. T. (2001) *J. Biol. Chem.* **276,** 35368–35374
13. Matunis, M. J., Wu, J., and Blobel, G. (1998) *J. Cell Biol.* **140,** 499–509
14. Rodriguez, M. S., Dargemont, C., and Hay, R. T. (2001) *J. Biol. Chem.* **276,** 12654–12659
15. Sampson, D. A., Wang, M., and Matunis, M. J. (2001) *J. Biol. Chem.* **276,** 21664–21669
16. Bernier-Villamor, V., Sampson, D. A., Matunis, M. J., and Lima, C. D. (2002) *Cell* **108,** 345–356
17. VanDemark, A. P., and Hill, C. P. (2002) *Curr. Opin. Struct. Biol.* **12,** 822–830
18. Walden, H., Podgorski, M. S., and Schulman, B. A. (2003) *Nature* **422,** 330–334
19. Cook, W. J., Jeffrey, L. C., Carson, M., Chen, Z., and Pickart, C. (1992) *J. Biol. Chem.* **267,** 16467–16471
20. Varadan, R., Walker, O., Pickart, C., and Fushman, D. (2002) *J. Mol. Biol.* **324,** 637–647
21. Varadan, R., Assfalg, N., Haririnia, A., Raasi, S., Pickart, C., and Fushman, D. (2004) *J. Biol. Chem.* **279,** 7055–7063
22. Rudolph, M. J., Wuebbens, M. M., Rajagopalan, K. V., and Schindelin, H. (2001) *Nat. Struct. Biol.* **8,** 42–46
23. Rudolph, M. J., Wuebbens, M. M., Turque, O., Rajagopalan, K. V., and Schindelin, H. (2003) *J. Biol. Chem.* **278,** 14514–14522
24. Bencsath, K. P., Podgorski, M. S., Pagala, V. R., Slaughter, C. A., and Schulman, B. A. (2002) *J. Biol. Chem.* **277,** 47938–47945
25. McIntosh, L. P., and Dahlquist, F. W. (1990) *Q. Rev. Biophys.* **23,** 1–38
26. Bayer, P., Arndt, A., Metzger, S., Mahajan, R., Melchior, F., Jaenicke, R., and Becker, J. (1998) *J. Mol. Biol.* **280,** 275–286
27. Jin, C., Shiyanova, T., Shen, Z., and Liao, X. (2001) *Int. J. Biol. Macromol.* **28,** 227–234
28. Sattler, M., Schleucher, J., and Griesinger, C. (1999) *Prog. NMR Spectrosc.* **34,** 93–158
29. Liu, Q., Jin, C., Liao, X., Shen, Z., Chen, D. J., and Chen, Y. (1999) *J. Biol. Chem.* **274,** 16979–16987
30. Farrow, N. A., Muhandiram, R., Singer, A. U., Pascal, S. M., Kay, C. M., Gish, G., Shoelson, S. E., Pawson, T., Foreman-Kay, J. D., and Kay, L. E. (1994) *Biochemistry* **33,** 5984–6003
31. Delaglio, F., Grzesiek, S., Vuister, G. W., Zhu, G., Pfeifer, J., and Bax, A. (1995) *J. Biomol. NMR* **6,** 277–293
32. Goddard, T. D., and Kneeler, D. G. (1999) *SPARKY 3*, University of California, San Francisco
33. Dosset, P., Hus, J.-C., Blackledge, M., and Marion, D. (2000) *J. Biomol. NMR* **16,** 23–28
34. Kay, L. E., Torchia, D. A., and Bax, A. (1989) *Biochemistry* **28,** 8972–8979
35. Wagner, G. (1997) *Nat. Struct. Biol.* **4,** (suppl.) 841–844
36. Tatham, M. H., Kim, S., Yu, B., Jaffray, E., Song, J., Zheng, J., Rodriguez, M. S., Hay, R. T., and Chen, Y. (2003) *Biochemistry* **42,** 9959–9969
37. Lin, D., Tatham, M. H., Yu, B., Kim, S., Hay, R. T., and Chen, Y. (2002) *J. Biol. Chem.* **277,** 21740–21748
38. Uchimura, Y., Nakao, M., and Saitoh, H. (2004) *FEBS Lett.* **564,** 85–90
39. Mossessova, E., and Lima, C. D. (2000) *Mol. Cell* **5,** 865–876
40. Wood, L. D., Irvin, B. J., Nucifora, G., Luce, K. S., and Hiebert, S. W. (2003) *Proc. Natl. Acad. Sci. U. S. A.* **100,** 3257–3262
41. Kamitani, T., Kito, K., Nguyen, H. P., Wada, H., Fukuda-Kamitani, T., and Yeh, E. T. (1998) *J. Biol. Chem.* **273,** 26675–26682
42. Desterro, J. M., Rodriguez, M. S., and Hay, R. T. (1998) *Mol. Cell* **2,** 233–239
43. Fuchs, S. Y., Lee, C. G., Pan, Z. Q., and Ronai, Z. (2002) *Cell* **110,** 531
44. Yang, S. H., and Sharrocks, A. D. (2004) *Mol. Cell* **13,** 611–617
45. Hardeland, U., Steinacher, R., Jiricny, J., and Schar, P. (2002) *EMBO J.* **21,** 1456–1464
46. Schwede, T., Kopp, J., Guex, N., and Peitsch, M.C. (2003) *Nucleic Acids Res.* **31,** 3381–3385